Islamic Azad University

Journal of
Optoelectronical Nanostructures

Summer 2023 / Vol. 8, No. 3

Research Paper

Designing an InGaP/InAlGaP Double Junction Solar Cell without an Anti-Reflection Coating by Adding a New Window Layer in the Upper Junction and Optimizing the Back Surface Field Layer

Neda Hasanzadeh Bishegahi[1], Abdollah Eskandarian[2], Abbas Ghadimi*[,3], Ali Esmaeeli[4]

[1,2,4] Department of Electrical Engineering, Rasht Branch, Islamic Azad University, Rasht, Iran

[3] Department of Electrical Engineering, Lahijan Branch, Islamic Azad University, Lahijan, Iran

Received: 18 Jul. 2023
Revised: 26 Aug. 2023
Accepted: 4 Sep. 2023
Published: 15 Sep. 2023

Use your device to scan and read the article online

Keywords:
Anti-Reflection Coating, Back Surface Field Layer, InGaP/InAlGaP, Upper Junction

Abstract:
The present study proposes a novel indium gallium phosphide/aluminum gallium indium phosphide (InGaP/InAlGaP) double junction solar cell without an anti-reflection coating that includes an upper InGaP cell, a lower InAlGaP cell, and a gallium arsenide (GaAs) tunnel junction. To increase the efficiency of the cell, a new window layer was used at the upper junction. To achieve higher efficiency, the researchers also optimized the back surface field layer of the lower cell. The results were analyzed via numerical modeling with Silvaco/Atlas software under the AM1.5 radiation spectrum. Findings suggested that using the sun=1 parameter, the obtained maximum values of short-circuit current, open-circuit voltage, fill factor, and efficiency parameters for the proposed solar cell structure were Jsc = 24.078 mA/cm2, Voc = 3.41886, FF = 91.1836, and Eff = 71.721%, respectively.

Citation: Neda Hasanzadeh, Abdollah Eskandarian, Abbas Ghadimi, Ali Esmaeeli. Designing an InGaP/InAlGaP Double Junction Solar Cell Without an Anti-Reflection Coating by Adding a New Window Layer in the Upper Junction and Optimizing the Back Surface Field Layer. **Journal of Optoelectronical Nanostructures.** 2023; 8 (3): 19-40. **DOI: 10.30495/JOPN.2023.31721.1285**

***Corresponding author:** Abbas Ghadimi
Address: Department of Electrical Engineering, Lahijan Branch, Islamic Azad University, Lahijan, Iran. **Tell:** 00989113413847 **Email:** aghadimi@gmail.com

1. INTRODUCTION

A rise in fuel prices, environmental issues, and fossil resource scarcity are factors driving industrialized countries to seek alternative energy sources to fossil fuels [1, 29]. A renewable energy alternative to fossil fuels is solar energy, which is the world's largest source of energy [2, 30]. When utilizing solar energy, it is crucial to take various factors, such as the photovoltaic effect, into account [31, 32]. The photovoltaic effect occurs when light strikes a material, resulting in voltage and current generation [3, 30].

Multi-junction solar cells are constructed from single cells with different band gaps [4, 5]. They absorb a broad spectrum of light and convert it to energy using the photovoltaic effect [3]. In simpler terms, photons are absorbed differently depending on the layer by utilizing semiconductors with different band gaps, such as indium gallium phosphide (InGaP) and gallium arsenide (GaAs) [6]. Because of their crystal lattice matching, direct band gap, and high absorption rates, InGaP and GaAs are ideal materials for making multi-junction solar cells [7, 8]. The simplest case for this structure is when two cells are arranged in succession [7, 8]. Multi-junction solar cells have a higher absorption capacity than single-junction cells [9].

Several studies have been conducted on methods and ways to enhance the efficiency of multi-junction solar cells. These studies dealt with the investigation of cell behavior indicators, cell geometry, and materials employed in such structures [9]. Among the effective factors in increasing the efficiency and performance parameters of multi-junction solar cells are the optimization and use of different materials and their effects in the tunnel area, the back surface field (BSF) layers, and the window layer [9–15]. Arzbin and Ghadimi [16] and Abbasian and Sabbaghi-Nadooshan [17] studied the effect of applying an anti-reflective coating on the efficiency of dual-junction solar cells. Other researchers added a thin layer of optimized carbon nanotubes to increase efficiency [18]. One of the reasons for poor solar cell performance is the carrier recombination speed between the window and the emitter surface. Some investigations were conducted on this layer using optimization and changing the type of material employed [13, 19].

In multi-junction solar cells, carrier recombination occurs on the cell surface in addition to the middle parts of each cell. In this case, this recombination can be reduced by adding a window layer that prevents minority carriers from reaching the cell surface. This layer acts as a limiting layer due to its high band gap and increases the efficiency of the solar cell. Since the window layer is an effective layer that helps increase the absorption of sunlight, this study aimed to improve the efficiency of an indium gallium phosphide/aluminum gallium indium

phosphide (InGaP/InAlGaP) double junction solar cell without an anti-reflection coating by using a new window layer in the upper junction and optimizing the BSF layer in the lower junction. Calculations were made about how well the proposed cell would work, and the results were compared to those of other structures that had been proposed.

2. THE PROPOSED SOLAR CELL MODELING AND SIMULATION STEPS

InGaP/InAlGaP Apparatus Structure

Simulation tools can be utilized by engineers to predict the real-world behavior of parts prior to their manufacturing [33]. Consequently, there is a reduction in both monetary and time-related expenditures. Silvaco/Atlas is a simulation program that can be utilized in the design of solar cells to demonstrate anticipated outcomes prior to the manufacturing process. This software conducts an analysis of the structure of the solar cell under consideration by employing a range of mathematical models, including Poisson's equation, the carrier continuity equation, the drift-diffusion model (DDM), the energy balance transfer model, as well as the LUMINOUS, OPTR, CONMOB, and SRH models. The solar cell configuration proposed in the present study consists of three distinct components, namely the upper InGaP cell, the lower InAlGaP cell, and the GaAs tunnel junction.

Each of the top and bottom cells has a window, base, emitter, and BSF layer. The first layer in multi-junction solar cells is the window layer. This layer has a high band gap and acts as a transparent coating on the emitter layer. It also absorbs the maximum amount of radiant light for the cell. Decreasing the recombination speed of the surface charges, reducing the series resistance of the cell, separating the electrons and holes that are near the junction before recombining, and conducting the radiated light to the lower layers are some of the main functions of this layer [20, 21].

Each individual cellular unit is equipped with a central p-n junction, known as the base layer and emitter layer. The aforementioned intersection serves as the locus of current production within a solar cell featuring multiple junctions. This region exhibits a significant degree of photon absorption. Upon the incidence of photons at the junction, a consequential generation of electron-hole pairs ensues, thereby instigating an output current through the segregation of the aforementioned electrons and holes at the junction [22, 23]. The implementation of BSF layers within cellular structures serves to mitigate the effects of carrier recombination and scattering that may arise between the base region and the upper cell's tunnel junction or between the emitter and the lower cell's tunnel junction. Through the incorporation of BSF layers, a formidable impediment is established

for the minority carriers within the base layer, effectively obstructing their recombination. The presence of a substantial amount of doping within these layers is notable. Through the establishment of an electric field between the metal contacts and the central p-n junction of each cell, the minority carriers are effectively repelled from the contacts. This results in a reduction of recombination, thereby increasing the current and voltage of the device, as evidenced by prior research [22, 23].

The tunnel layer is one of the most important parts of a multi-junction cell and is placed as an interface between the upper and lower cells. This layer creates a path with low resistance for the flow of charge carriers [12]. Because there is a lot of doping in the tunneling region, its width is smaller than that of a normal p-n junction. This makes it possible for electrons to pass through the potential barrier, which creates a current [9]. In the proposed model of the present study, the upper cell had two window layers, which reduced the recombination of surface charges over a wider range. On the other hand, by optimizing the BSF layer, the scattering of carriers toward the tunnel junction was reduced, and finally, the efficiency of the solar cell increased. Table I shows the proposed dual-junction solar cell based on InGaP/InAlGaP materials. The doping and thickness of each layer are also listed.

Table I
The proposed dual-junction solar cell based on InGaP/InAlGaP materials

0.03µm	Window	InAlGaP	p=2e18cm^{-3}
0.40µm	Window	InAlGaP	p=2e17cm^{-3}
0.05 µm	Emitter	InGaP	p=2e18cm^{-3}
0.55 µm	Base	InGaP	n=7e16cm^{-3}
0.03 µm	BSF	InAlGaP	n=2e17cm^{-3}
0.03 µm	BSF	InAlGaP	n=2e18cm^{-3}
0.025 µm	Tunnel	GaAs	n=5e19cm^{-3}
0.025 µm	Tunnel	GaAs	p=3e19cm^{-3}
0.04 µm	Window	InGaP	p=2e18cm^{-3}
0.5 µm	Emitter	InAlGaP	p=3e18cm^{-3}
3.0 µm	Base	InAlGaP	n=2e17cm^{-3}
2.0 µm	BSF	InAlGaP	n=5e18cm^{-3}
0.2µm	Sub	GaAs	n=1e18cm^{-3}

Selection and Properties of Materials Used in the Proposed Dual-junction Solar Cell

The selection of materials for each subcell was determined by the crystal lattice constant matching condition, current matching, and optoelectronic characteristics. In order to have a crystal lattice of the desired quality, materials with close lattice constants were used.

Failure to match the crystal lattice of any material or other growth defects will reduce the efficiency and electronic characteristics of the device. In other words, points with crystal defects cause recombination and the loss of light-produced minority carriers, which reduce the photovoltaic effect of devices [9, 19]. Current matching is another important factor in multi-junction solar cells. According to Kirchhoff's current law, since the sub-cells are connected in series, a similar current passes through the junction. In this case, the total current of the multi-junction solar cell is limited to the minimum current of the sub-cells. The produced current is also dependent on the number of photons with energy greater than the band gap, the thickness of the layers, the photogeneration rate, and the absorption coefficient of the materials used in each layer. The correlation between the intensity of incoming light and the quantum of photons absorbed by the cell is directly proportional. Since the upper cell absorbs a significant portion of the sun's spectrum, it is necessary to choose a material for the window layer that has a high band gap and a suitable thickness to produce current matching [16, 24]. Finally, the use of materials with a high absorption coefficient, increasing the lifetime of minority carriers and increasing mobility, increases the optoelectronic performance of the device [25,34].

In our proposed structure, InAlGaP material was used due to its high band gap and the limiting property of the recombination speed of surface charges in the new window layer.

Adding A New Window Layer

The window layer facilitates the augmentation of minority carriers and their channeling towards the junction in multi-junction solar cells. In this particular scenario, electrons and holes produced by light undergo segregation via the p-n junction. Through the implementation of an auxiliary domain, the minority carriers are efficiently transported towards the p-n junction by means of the BSF layer, thereby reducing surface recombination. Consequently, the device's short-circuit current and optical power exhibit an increase [10]. Our proposed structure has been optimized through the incorporation of a new window layer composed of InAlGaP, which possesses a bandgap of 2.3 eV. This has allowed us to determine the ideal doping amount and thickness for our structure. The values

extracted from Silvaco/Atlas software for the three distinct types of doping are presented in Tables IIa–IIc.

Table IIa
The changes applied to the new window layer with doping accept $= 2e^{17}$

thickness(um)	Js(mA/cm2)	Voc(v)	FF(%)	Eff(%)
0/1	21.0242	3.39997	91.4042	62.4275
0/2	22.7282	3.40077	91.4385	67.5284
0/3	23.5881	3.40008	91.2585	69.9311
0/4	24.0781	3.39864	90.7533	70.9586
0/5	23.4961	3.3969	91.3173	69.6381
0/6	21.6555	3.39505	92.6635	65.0936

Table IIb
The changes applied to the new window layer with doping accept $= 2e^{18}$

thickness(um)	Jsc(mA/cm2)	Voc(v)	FF(%)	Eff(%)
0/1	16.3385	3.38974	91.2893	48.3074
0/2	16.0594	3.38666	91.498	47.5475
0/3	16.1795	3.38474	91.6083	47.9336
0/4	16.4306	3.38322	91.6485	48.6771
0/5	16.7085	3.38184	91.6055	49.4569
0/6	16.9706	3.38048	91.4811	50.1444
0/7	17.1987	3.37895	91.2467	50.6652
0/8	17.3868	3.37731	90.7714	50.9278
0/9	17.1534	3.37566	90.7847	50.2269
1	15.9269	3.37401	92.3694	47.4265
1/1	14.81	3.37235	92.9988	44.3793
1/2	13.7907	3.3707	93.3767	41.4725

The comparison of the obtained values shows that the absorption of photons increased effectively with a thickness of 400 nm and a doping of $p = 2e^{17}\ cm^{-3}$. On the other hand, a stronger potential barrier was created for the dispersion of minority carriers towards the junction, in which case the efficiency of the double-junction solar cell reached a maximum of 70.9586%. Figure 1 shows the efficiency relative to the thickness of the new window layer and the appropriate doping in the upper cell.

Table IIc
The changes applied to the new window layer with doping accept = $2e^{19}$

thickness(um)	Jsc(mA/cm^2)	Voc(v)	FF(%)	Eff(%)
0/1	14.1369	3.38368	91.1528	41.6609
0/2	14.2007	3.38174	91.4169	41.9461
0/3	14.5451	3.38061	91.5843	43.0277
0/4	14.9596	3.37961	91.6622	44.2784
0/5	15.3638	3.37849	91.664	45.4606
0/6	15.7282	3.3773	91.5974	46.4887
0/7	16.0412	3.37603	91.4467	47.318
0/8	16.3018	3.37468	91.1568	47.9151
0/9	16.5116	3.37327	90.5042	48.1642
1	15.9265	3.37181	91.4659	46.9308
1/1	14.8099	3.37033	92.5934	44.159
1/2	13.7907	3.36863	93.1236	41.3347

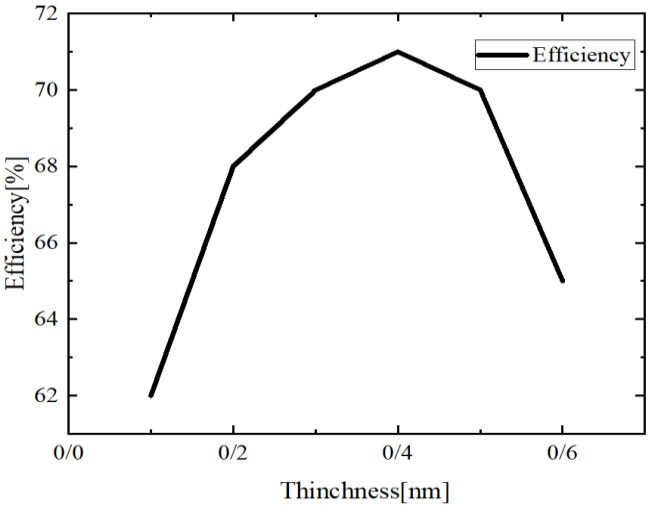

Fig. 1. The efficiency plot with respect to the thickness of the window layer in the upper cell.

Changing the Thickness of the BSF Layer of the Lower Cell

The BSF layer was one of the most significant layers in determining the efficiency of our proposed solar cell. The minority carriers that were moving toward the junction concentrated in the window layer. However, some of them tended to scatter in the opposite direction and move toward the back surface of the cell. To prevent this, very thin layers with high concentrations (the BSF layers) were made at the bottom of the cells. By forming an electrostatic field and a barrier against minority carriers, these layers stopped carriers from scattering toward the tunnel junction. This reduced surface recombination rates. Also, using two layers of BSF would help create an additional field around the junction and reduce the carrier recombination rate [25, 26]. At this stage, new results were obtained in the proposed structure by optimizing one of the BSF layers in the lower junction. As shown in Table III, the efficiency was maximized for the lower cell because of the improvement in performance parameters at 200 nm thickness.

Table III
The efficiency values obtained with various values for the BFS layer thickness in the lower cell

thickness(um)	Jsc(mA/cm^2)	Voc(v)	FF(%)	Eff(%)
0/5	24.0781	3.39864	90.7533	70.9586
1	24.0784	3.40999	90.9908	71.3828
1/5	24.0786	3.41534	91.1085	71.5878
2	24.0787	3.41886	91.1836	71.721
2/5	24.0788	3.42118	91.2328	71.8087
3	24.0789	3.42281	91.2822	71.8821
3/5	24.0789	3.42407	91.3185	71.9371

3. SIMULATION RESULTS AND DISCUSSION

In this study, the proposed structure was simulated under the AM 1.5G and sun 1000 standard spectra. The diagram of the spectrum function drawn by the Silvaco/Atlas simulator is shown in Figure 2. QTY.MESH and QTX.MESH were used to determine the mesh in horizontal and vertical directions. Figures 3 and 4 show meshing and doping in different layers of the proposed solar cell.

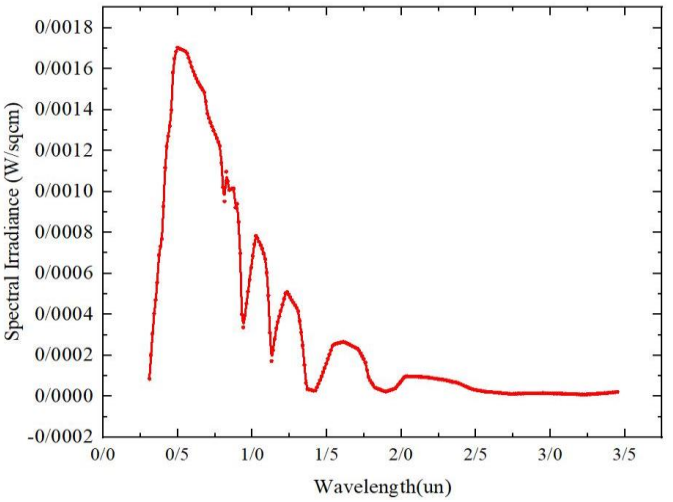

Fig. 2. The standard AM 1.5G spectrum used in the simulation of the proposed solar cell structure.

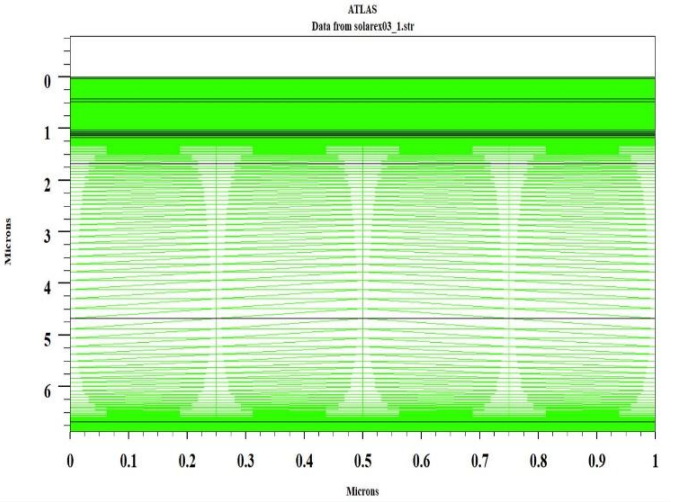

Fig. 3. The meshing of the proposed dual-junction solar cell structure.

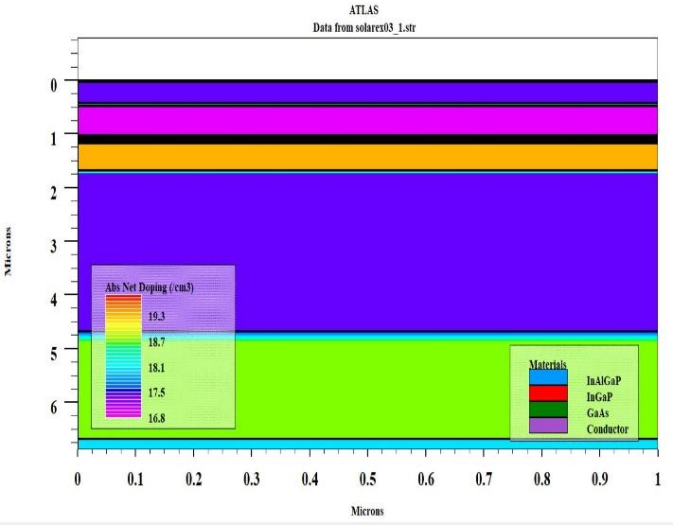

Fig. 4. The doping of the various layers used in the proposed solar cell structure.

Figure 5 shows the structure of the proposed double junction solar cell, separated by different layers.

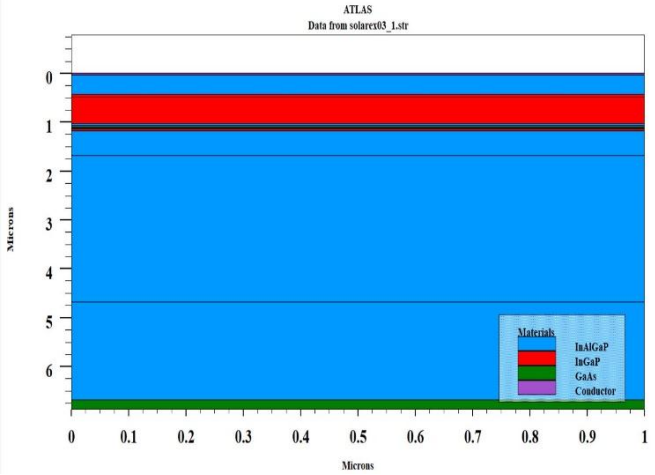

Fig. 5. The structure of the proposed dual-junction solar cell.

In what follows below, the results of the simulation of the proposed model using the Silvaco/Atlas simulator are presented in Figures 6–12. The photogeneration rate, which indicates the number of photons produced in each

layer, is a critical parameter in determining the efficiency of a multi-junction solar cell. Figure 6 shows the photogeneration rate in different layers of our proposed solar cell. Since the proposed cell works over a wide range of wavelengths, it can be said that the photogeneration in solar cells depends solely on the photovoltaic properties of the material. The value of this rate is calculated from equation (1):

$$G = \eta_0 \frac{p\lambda}{hc} \alpha e^{-\alpha y} \tag{1}$$

where G is the photogeneration rate, p is the cumulative effect of reflection, transmission, and loss due to the absorption of radiation, y is the relative distance of a given ray, η_0 is the internal quantum efficiency, h is Plank's constant, λ is the wavelength, c is the speed of light, and α is the absorption coefficient calculated for each pair (n, k) using the following equation (2) [13, 14]:

$$\alpha = \frac{4\pi k}{\lambda} 10^7 \, cm^{-1} \tag{2}$$

Figure 6 shows details of the photogeneration rate in different layers. The photogeneration rate was higher at the surface of the cell, where most sunlight was received. Considering that there was an accumulation of charge carriers near the BSF layer, the light production rate was also at its maximum in this layer.

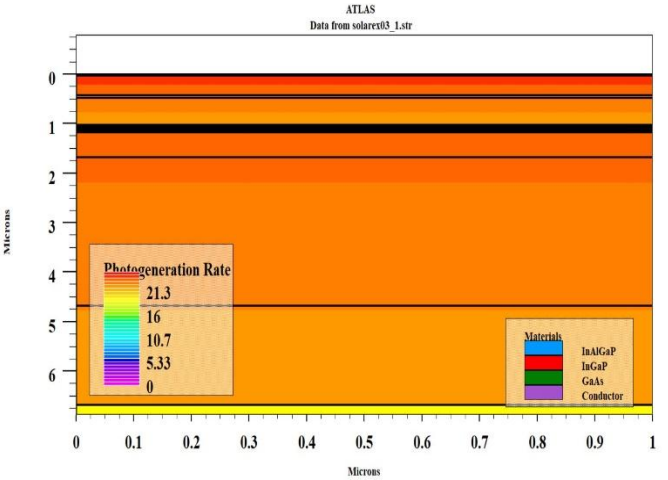

Fig. 6. The photogeneration rate in different layers of the proposed solar cell structure.

The diagram of the energy band of the proposed solar cell at zero bias is shown in Figure 7. The new window layer added to the upper cell created a potential barrier against minority carriers in the emitter layer. The bandgap and quality of the material used in the window layer must have been selected in a way that would reduce the effect of surface recombination. In our proposed structure, InAlGaP with a bandgap of 2.3 eV was used in the new window layer. The BSF layers also created a potential barrier that prevented the minority carriers of the base layer from recombining. These layers attempted to provide maximum photon transparency while also assisting photons in reaching the lower cell.

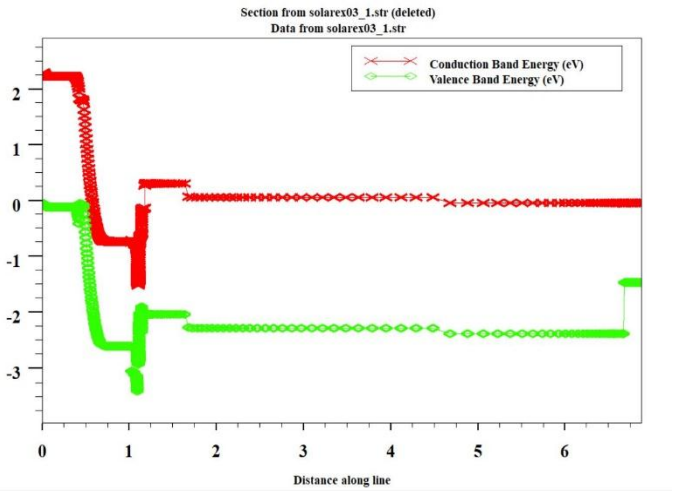

Fig. 7. The energy band diagram of the proposed solar cell.

Figure 8 presents the potential distribution of each layer of the proposed cell. Due to the existence of an internal built-in potential during the formation of p-n junctions, the highest voltage drop occurred in the discharge areas related to p-n junctions.

Figures 8 and 9 show the distribution of the electric field in different layers of our proposed solar cell structure. Because of the appearance of the voltage drop across the junction as a result of the built-in potential inside the structure, the electric field was generally higher in the junction area [15, 23].

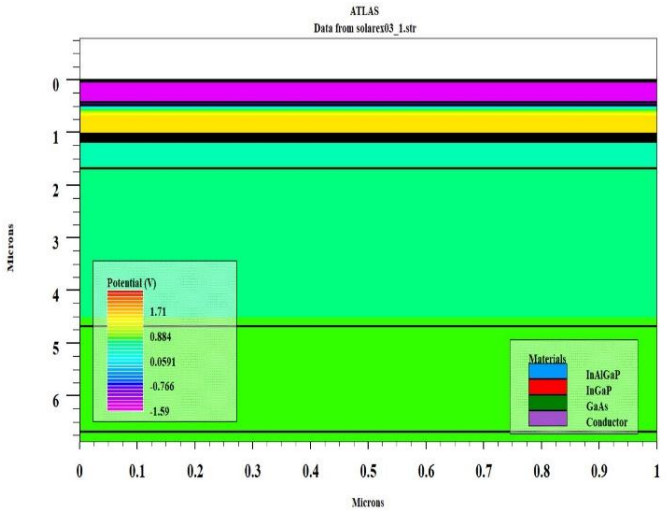

Fig. 8. The distribution of potential in each layer of the proposed solar cell structure.

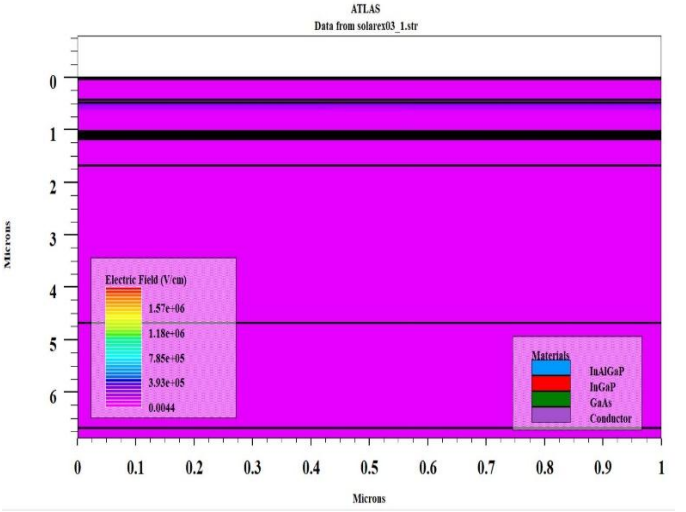

Fig. 9. The distribution of the electric field in each layer of the proposed solar cell structure.

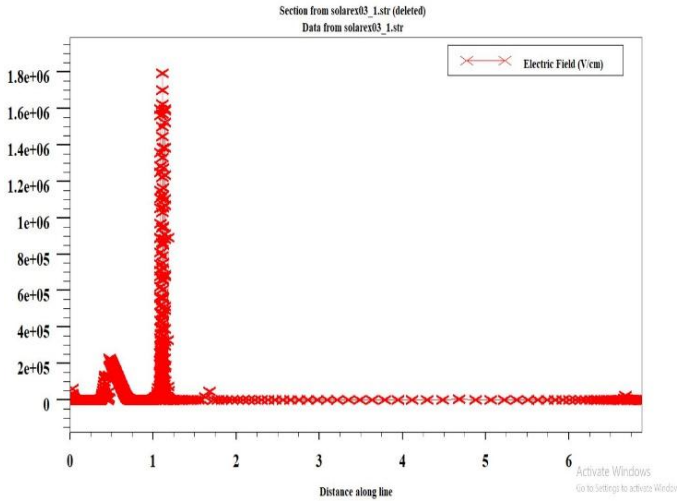

Fig. 10. The electrical field at the junction region of the proposed solar cell structure.

Quantum efficiency and spectrum response are additional elements that must be considered while analyzing solar cells. Figure 11 shows the spectral response curve of our proposed cell. The spectral response was composed of three light currents: the light source current (photocurrent source), the available light current (photocurrent), and the cathode current. The light current (photocurrent) source indicates the number of emitted photons. In our proposed solar cell, the absorbed photons made up the available light current (photocurrent), and the cathode current controlled the output current of the absorbed photons. The spectral response was conceptually similar to quantum efficiency. Figure 12 shows the quantum efficiency diagram of our proposed cell, which shows the number of electrons output from the solar cell compared to the number of photons in the device [17, 21, and 28].

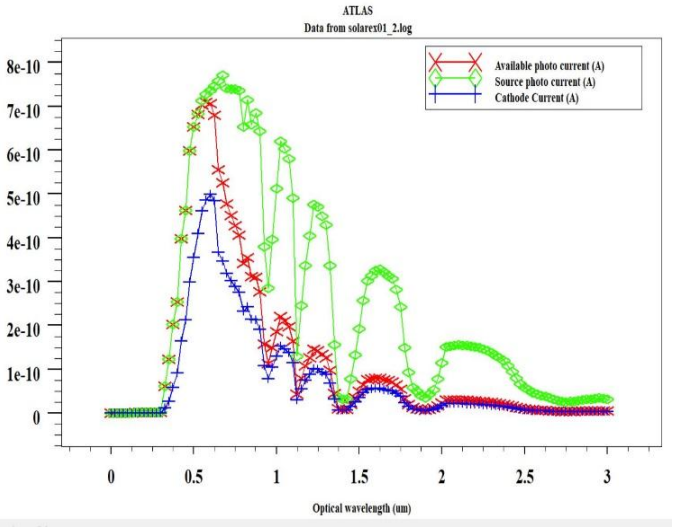

Fig. 11. Spectral response curve of the proposed solar cell structure.

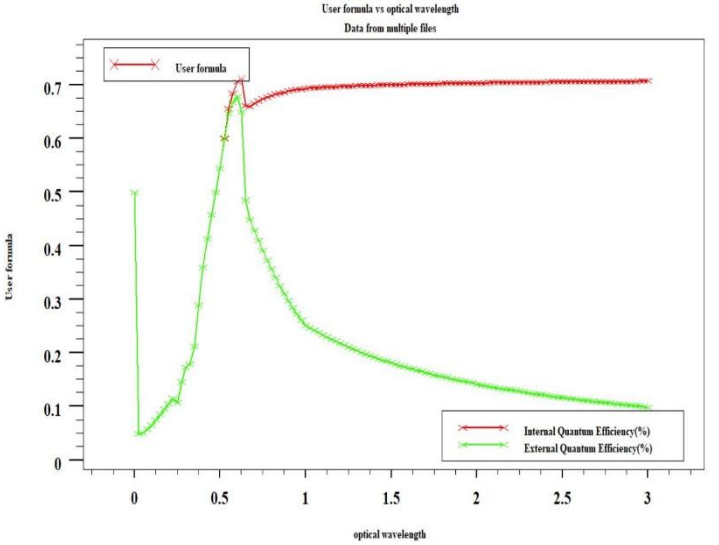

Fig. 12. Quantum efficiency curve of the proposed solar cell structure.

4. COMPARING THE RESULTS

The voltage-current diagram of our proposed optimized model is shown in Figure 14. As can be seen, the current increased significantly after applying the changes.

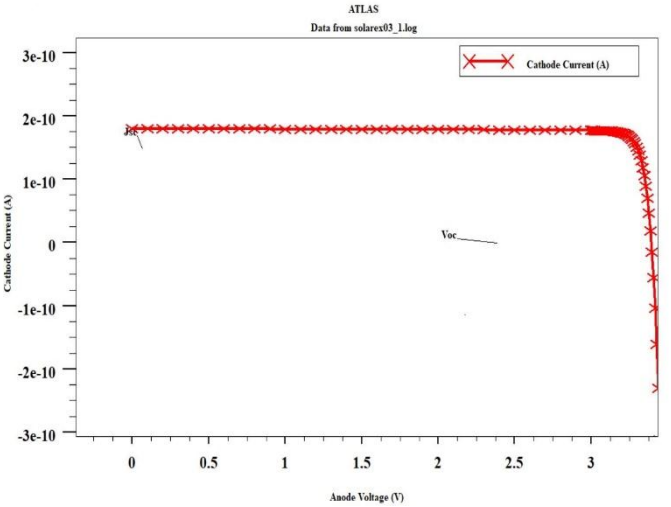

Fig. 13. The current-voltage plot of the proposed model.

In Table IV, the values obtained from our proposed cell show that the double-junction InGaP/InAlGaP solar cell without anti-reflection coating with a new window layer and optimization of the lower BSF layer was more efficient compared to the model presented by Nayak et al. [23].

Table IV
Comparing our proposed double-junction InGaP/InAlGaP solar cell with Nayak et al. [23]

Solar cells	Spectrumsun	sun	J_{SC}(mA/cm2)	V_{OC}(V)	FF(%)	Efficiency(%)
ref [21]	Am1.5	1000	1761.9	3.73	92.14	60.5452
Our proposed mod	Am1.5	1	24.0787	3.41886	91.1836	71.721

The parameters obtained from the simulation of the proposed structure were also compared with those of prior studies. Table V provides these results.

Table V
Comparing the parameters of the proposed cell structure with those of prior studies for AM 1.5G spectrum

Solar cells	Spectrumsun	sun	VOC(V)	JSC(mA/cm2)	FF(%)	Efficiency(%)
Lueck et al. [11]	AM1.5G	1.0	2.23	1.09E-10	79.00	23.6
Leem et al. [12]	AM1.5G	1.0	2.30	1.06E-10	87.55	25.14
Singh & Sarkar [13]	AM1.5G	1000	2.66	1.06E-8	89.50	36.67
Nayak et al. [23]	AM1.5G	1000	2.66	1.733E-8	66.67	39.15
Dutta et al. [15]	AM1.5G	1000	2.668	1.823E-8	88.29	40.879
Sahoo et al. [21]	AM1.5G	1000	2.7043	1.898E-8	88.88	43.603
Abbasian [17]	AM1.5G	1.0	3.347	1.759E-10	90.90	53.51
Abbasian [17]	AM1.5G	1000	3.7304	1.7619E-7	92.14	60.5452
Arzbin [18]	AM1.5G	1.0	2.522	29.09	88.49	62.04
The proposed model of the present study	AM1.5G	1.0	3.41886	24.0787	91.1836	71.721

5. CONCLUSIONS

In this paper, we present a novel design of a double junction solar cell structure Without an Anti-Reflection Coating by Adding a New Window Layer in the Upper Junction and Optimizing the Back Surface Field Layer. Considering that solar cells will be a viable alternative to fossil fuels in the future, increasing the efficiency and improving the parameters of solar cells, along with reducing construction costs, is one of the most important goals of researchers in this field. In the present study, in order to optimize the efficiency of our proposed solar cell, a new window layer was used at the upper junction. In addition, the BSF layer of the lower cell was also optimized. The parameters of open circuit voltage, short circuit current, fill factor, and efficiency in the proposed structure were extracted using the Silvaco/Atlas software simulation. The AM 1.5 G spectrum, $sun = 1$, and $J_{sc} = 24.0787\ mA/cm^2$ parameters were used in the simulations executed. The following outcomes were obtained from these simulations: $V_{oc} = 3.41886\ V$, $FF = 91.1836$, and $Eff = 71.721\%$, indicating the efficiency of our proposed solar cell structure.

REFERENCES

[1] Rabbi MF, Popp J, Máté D, Kovács S. *Energy Security and Energy Transition to Achieve Carbon Neutrality*. Energies. 15(21) (2022,Oct) 1-18. Available: https://www.mdpi.com/1996-1073/15/21/8126

[2] Kharchich FZ, Khamlichi A. *Optimizing efficiency of InGaP/GaAs dual-junction solar cells with double tunnel junction and bottom back surface field layers*. Optik. 272(1) (2023,Feb) 170196. Available: https://www.sciencedirect.com/science/article/abs/pii/S0030402622014541

[3] Zhang S, Sun J. *Design and optimization of ARC solar cell with intrinsic layer and p–n junction in bottom cell under AM1. 5G standard spectrum*. Emergent Materials. 6(1) (2023,Jan) 159-166. Available: https://link.springer.com/article/10.1007/s42247-023-00457-4

[4] Arijit.B. R, Mandla.M, Roshika.K: *Performance enhancement Of GaAs and InP Based Multi-Junction Silicon Solar Cells using thickness and doping profile optimization*, in Chennai, India. IEEE, (2023) 19-21. Available: https://ieeexplore.ieee.org/abstract/document/10134102

[5] Goetzberger A, Luther J, Willeke G. *Solar cells: past, present, future. Solar energy materials and solar cells.*74(1) (2002,Oct) 1-11. Available: https://www.sciencedirect.com/science/article/abs/pii/S0927024802000429

[6] Bakour A, Saadoune A, Bouchama I, Dhiabi F, Boudour S, Saeed MA. *Effect and optimization of ZnO layer on the performance of GaInP/GaAs tandem solar cell.* Micro and Nanostructures.168(1) (2022, Aug) 207294. Available: https://www.sciencedirect.com/science/article/abs/pii/S2773012322001078

[7] Peng YS, Yao MH, Liu ZM, Tu JL, Cao QJ, Gong SF, Hu YT, Zhou SL. *Numerical investigation on performance of ultra-thin GaAs solar cells enabled with frontal surface pyramid array*. Journal of Physics D: Applied Physics. 24(55) (2022, Mar) 245105. Available: https://iopscience.iop.org/article/10.1088/1361-6463/ac5da3/meta

[8] Luque A, Hegedus S, editors. *Handbook of photovoltaic science and engineering*. John Wiley & Sons. (2011, Mar). Available: https://kashanu.ac.ir/Files/Content/Handbook.pdf

[9] Hutchby JA, Markunas RJ, Bedair SM. *Material aspects of the fabrication of multijunction solar cells*. Photovoltaics.543(9) (1985, May) 40-61. Available: https://www.spiedigitallibrary.org/conference-proceedings-of-spie/0543/0000/Material-Aspects-Of-The-Fabrication-Of-Multijunction-Solar-Cells/10.1117/12.948195.short?SSO=1

[10] De Vos A. *Detailed balance limit of the efficiency of tandem solar cells*. Journal of Physics D: Applied Physics.13(5) (1980, May) 839. Available: https://iopscience.iop.org/article/10.1088/0022-3727/13/5/018/meta

[11] Lueck MR, Andre CL, Pitera AJ, Lee ML, Fitzgerald EA, Ringel SA. *Dual junction GaInP/GaAs solar cells grown on metamorphic SiGe/Si substrates with high open circuit voltage*. IEEE Electron Device Letters.27(3) (2006, Feb) 142-144. Available: /https://ieeexplore.ieee.org/abstract/document/1599460

[12] Leem JW, Lee YT, Yu JS. *Optimum design of InGaP/GaAs dual-junction solar cells with different tunnel diodes.* Optical and quantum electronics. 41(8) (2009,Jun) 605-12. Available: https://link.springer.com/article/10.1007/s11082-010-9367-1

[13] Singh KJ, Sarkar SK. *Highly efficient ARC less InGaP/GaAs DJ solar cell numerical modeling using optimized InAlGaP BSF layers. Optical and Quantum Electronics.*43(1) (2012, Feb) 1-21. Available: https://link.springer.com/article/10.1007/s11082-011-9499-y

[14] Nayak PP, Dutta JP, Mishra GP. *Efficient InGaP/GaAs DJ solar cell with double back surface field layer. Engineering Science and Technology, an International Journal.*18(3) (2015, Sep) 325-35. Available: https://www.sciencedirect.com/science/article/pii/S2215098615000245

[15] Dutta JP, Nayak PP, Mishra GP. *Design and evaluation of ARC less InGaP/GaAs DJ solar cell with InGaP tunnel junction and optimized double top BSF layer. Optik.*127(8) (2016, Apr) 4156-61. Available: https://www.sciencedirect.com/science/article/pii/S0030402616000905

[16] Arzbin H, Ghadimi A. *Efficiency improvement of ARC less InGaP/GaAs DJ solar cell with InGaP tunnel junction and optimized two BSF layer in top and bottom cells.* Optik. 148(1) (2017, Nov) 358-67. Available: https://www.sciencedirect.com/science/article/pii/S0030402617310744

[17] Abbasian S, Sabbaghi-Nadooshan R. *Design and evaluation of ARC less InGaP/AlGaInP DJ solar cell. Optik*.136(1) (2017,May) 487-96. Available: https://www.sciencedirect.com/science/article/pii/S0030402617302279

[18] Arzbin HR, Ghadimi A. *Improving the performance of a multi-junction solar cell by optimizing BSF, base and emitter layers*. Materials Science and Engineering: B. 243(1) (2019, Apr) 108-14. Available: https://www.sciencedirect.com/science/article/pii/S092151071930087X

[19] Bagheri S, Talebzadeh R, Sardari B, Mehdizadeh F. *Design and simulation of a high efficiency InGaP/GaAs multi junction solar cell with AlGaAs tunnel junction. Optik*.199(1) (2019, Dec) 163315. Available: https://www.sciencedirect.com/science/article/pii/S0030402619312136

[20] Chee KW, Hu Y. *Design and optimization of ARC less InGaP/GaAs single-/multi-junction solar cells with tunnel junction and back surface field layers*. Superlattices and Microstructures. 119(1) (2018, Jul) 25-39. Available: https://www.sciencedirect.com/science/article/pii/S0749603617329087

[21] Sahoo GS, Nayak PP, Mishra GP. *An ARC less InGaP/GaAs DJ solar cell with hetero tunnel junction*. Superlattices and Microstructures. 95(1) (2016, Jul 115-27. Available: https://www.sciencedirect.com/science/article/pii/S0749603616301975

[22] Ali K, Khan SA, MatJafri MZ. *TCAD design of silicon solar cells in comparison of antireflection coatings and back surface field*. Optik. 127(19) (2016, Oct) 7492-7. Available: https://www.sciencedirect.com/science/article/pii/S0030402616304314

[23] Nayak PP, Dutta JP, Mishra GP. *Performance Evaluation of InGaP/GaAs Solar Cell with Double Layer ARC*. InIntelligent Computing, Communication and Devices. Springer . 308(1) (2015,Jun) 553-9. Available: https://link.springer.com/chapter/10.1007/978-81-322-2012-1_59

[24] Farhadi B, Naseri M. *A novel efficient double junction InGaP/GaAs solar cell using a thin carbon nano tube layer*. Optik.127(15) (2016, Aug) 6224-31. Available: https://www.sciencedirect.com/science/article/pii/S0030402616303138

[25] Castaner L, Silvestre S. *Modelling photovoltaic systems using PSpice*. John Wiley and Sons: 2002, 21-174. Available: https://www.sciencedirect.com/science/article/pii/S0030402616303138

[26] Routray SR, Sahoo GS, Mishra GP. *Effect of intrinsic layer on the performance of InGaP/GaAs dual Junction solar cell*. Michael Faraday IET International Summit, (2015,Sep). Available: https://digital-library.theiet.org/content/conferences/10.1049/cp.2015.1655

[27] Miles RW. Photovoltaic solar cells: *Choice of materials and production methods. Vacuum*. 80(10) (2006, Aug) 1090-7. Available: https://www.sciencedirect.com/science/article/pii/S0042207X06000182

[28] Zhao XF, Aierken A, Heini M, Tan M, Wu YY, Lu SL, Hao RT, Mo JH, Zhuang Y, Shen XB, Xu Y. *Degradation characteristics of electron and proton irradiated InGaAsP/InGaAs dual junction solar cell.* Solar Energy Materials and Solar Cells.206(1) (2020, Mar) 110339. Available: https://www.sciencedirect.com/science/article/abs/pii/S0927024819306658

[29] S. M. S. Hashemi Nassab, M. Imanieh, and A. Kamaly. *The Effect of Doping and the Thickness of the Layers on CIGS Solar Cell Efficiency.* Journal of Optoelectronical Nanostructures. 1(1) (2016) 9-24. Available: https://jopn.marvdasht.iau.ir/article_1812.html

[30] Y. Sefidgar, H. Rasooli Saghai, and H. Ghatei Khiabani Azar. *Enhancing Efficiency of Two-bond Solar Cells Based on GaAs/InGaP*. Journal of Optoelectronical Nanostructures. 4(2) (2019) 83-102. Available: https://jopn.marvdasht.iau.ir/article_3480_0b715e5dbfb8c90033530e34eb33a84a.pdf

[31] M. Rajaee and S. Rabiee. *Analysis and Implementation of a New Method to Increase the Efficiency of Photovoltaic Cells by Applying a Dual Axis Sun Tracking System and Fresnel Lens Array.* Journal of Optoelectronical Nanostructures. 6(3) (2021) 59-80. Available: https://jopn.marvdasht.iau.ir/article_4981.html

[32] A. Keshavarz and Z. Abbasi. *Spatial soliton pairs in an unbiased photovoltaic-photorefractive crystal circuit*. Journal of Optoelectronical

Nanostructures. 1(1) (2016) 81-90. Available: https://jopn.marvdasht.iau.ir/article_1817_1ee4531eafbf20226b5f4158a81b8220.pdf

[33] A. Mirkamali and K. Muminov. *The effect of change the thickness on CdS/CdTe tandem multi-junction solar cells efficiency*. Journal of Optoelectronical Nanostructures. 2(3) (2017) 13-24. Available: https://jopn.marvdasht.iau.ir/article_2428_71d76f5443f30e4893971a3af3662275.pdf

[34] SN Jafari, A Ghadimi, S Rouhi, *Strained Carbon Nanotube(SCNT) thin layer effect on GaAs solar cells efficiency*. Journal of Optoelectronical Nanostructures. 5(4) (2020) 87-110. Available: http://jopn.miau.ac.ir/article_4505_8947f89a5f380e375d5e6425249c10b5.pdf